Rapid and Quantitative Displacement of Poly(ethylene oxide) from $MnPS_3$ and Other Layered Hosts

Christopher O. Oriakhi and Michael M. Lerner*

Department of Chemistry and Center for Advanced Materials Research, Oregon State University, Corvallis, Oregon 97331

Received February 5, 1996. Revised Manuscript Received May 28, 1996[⊗]

The reaction of tetraethylammonium salt with the nanocomposites $K_{0.2}(C_2H_4O)_{2.3}M_{0.9}PS_3$ (M = Mn, Cd) under ambient conditions results in the rapid and quantitative displacement of the polymer and alkali metal to form the alkylammonium intercalate. Solid reactants and products, characterized using XRD, TGA, IR, gel permeation chromatography, and elemental analyses, show that these displacement reactions go to completion with no polymer degradation after initial formation of the nanocomposite. Pseudoreaction rates (0.0−7.8 min^{-1}) are obtained using temporal XRD studies for different cations, concentrations, and polymer molecular weights. Reaction rates increase for lower polymer molecular weights, and a strong rate dependence is observed for alkylammonium concentration. Displacement from the MPS_3 host occurs very slowly, or only to a limited extent, for tetramethylammonium, tetrapropylammonium, and tetrabutylammonium salts. A reaction mechanism is proposed from observed trends. Rapid displacement is also reported for other layered nanocomposites containing poly(ethylene oxide) within Li_xMoS_2, Na−montmorillonite, and Li_xMoO_3.

Introduction

Considerable research activity has focused on the formation of two-dimensional materials comprised, at the nanoscale, of alternating layers of organic polymers and inorganic sheet structures. These materials can be described, depending on one's frame of reference, as intercalation compounds of polymers within layered hosts, or as nanocomposites of two solid phases. A principal reason for the recent interest in these materials lies in the thermochemical,[1] rheological,[2] electrical,[3] and optical[4] properties that can be realized in such assemblies. Along with new properties are the associated possibilities of exercising a greater control over the physical and chemical behavior of solids.

Although the enthalpic terms associated with forming intercalation compounds of small molecules and polymers may be similar, very different preparative strategies are generally required. The difference derives from the large size of polymer molecules, which kinetically limits a topotactic mechanism wherein molecules diffuse into an existing layered structure. Synthetic strategies that have been successfully employed to prepare polymer-containing nanocomposites include the following: (a) the in situ polymerization of small precursors that are first incorporated by a topotactic mechanism,[5,6] (b) the exfoliation of a layered inorganic structure, adsorption of a polymer onto the exposed surfaces from solution,[7,8] or emulsion,[9] and subsequent flocculation of nanocomposite, (c) melt intercalation where a polymer is heated above the glass transition,[10] and (d) the use of a polymer as a template for growth of the inorganic layers.[11,12]

Poly(ethylene oxide), $(C_2H_4O)_n$ [PEO], is employed commercially for a variety of applications,[13] and use in polymer electrolytes has been studied widely.[14] Advantages in using nanocomposites rather than bulk PEO can include changes in rheological and electrical properties.[15] Several reports have appeared on the formation of layered nanocomposites containing PEO or other poly- or oligoethers. The layered inorganic hosts studied include montmorillonite,[16] MoS_2,[1] TiS_2,[17] MoO_3,[18] and $MnPS_3$.[19] In each of these examples, at maximum polymer incorporation the PEO layers have dimensions of 8−9 Å along the stacking direction, which is consistent with a bilayer of the polymer adsorbed onto the encasing inorganic surfaces (Table 1). The polymer layers also contain alkali metal cations, which are solvated by PEO and compensate the negative charge of the inorganic layers.

Profound differences exist between nanocomposited and bulk crystalline PEO: for example, no melting transition is observed in the former case. In fact, little

[⊗] Abstract published in *Advance ACS Abstracts,* July 15, 1996.

(1) Lemmon, J.; Lerner, M. *Chem. Mater.* **1994**, *6*, 207.
(2) Lan, T.; Kaviratna, P. D.; Pinnavaia, T. J. *Chem. Mater.* **1994**, *6*, 1395.
(3) Aranda, P.; Ruiz-Hitzky, E. *Chem. Mater.* **1992**, *4*, 1395.
(4) Nicoud, J.-F. *Science* **1994**, *263*, 636.
(5) Kanatzidis, M. G.; Tonge, L. M.; Marks, T. J.; Marcy, H. O.; Kannewurf, C. R. *J. Am. Chem. Soc.* **1987**, *109*, 3797.
(6) Mehrotra, V.; Gianellis, E. *Solid. State. Ionics* **1992**, *51*, 115.
(7) Lemmon, J.; Wu, J.; Oriakhi, C.; Lerner, M. *Electrochim. Acta* **1995**, *40*, 2245.
(8) Nazar, L.; Zhang, Z.; Zinkweg, D. *J. Am. Chem. Soc.* **1992**, *114*, 6239.
(9) Oriakhi, C.; Lerner, M. *Mater. Res. Bull.* **1995**, *30*, 723.
(10) Vaia, R.; Vasudevan, S.; Krawiec, W.; Scanlon, L.; Giannelis, E. *Adv. Mater.* **1995**, *7*, 154.
(11) Martin, C. R. *Acc. Chem. Res.* **1995**, *28*, 61.
(12) Oriakhi, C. O.; Farr, I. V.; Lerner, M. M. *J. Mater. Chem.* **1996**, *6*, 103.
(13) Bailey, F. E.; Koleske, J. V. *Poly(ethylene oxide)*; Academic Press: New York, 1976.
(14) (a) Vincent, C. A. *Chem. Brit.* **1989**, 391. (b) Also see: *Polymer Electrolyte Reviews 1 and 2*; MacCaullum, J. R., Vincent, C. A., Eds.; Elsevier: New York, 1989.
(15) Aranda, P.; Ruiz-Hitzky, E. *Acta Polym.* **1994**, *45*, 59.
(16) Wu, J.; Lerner, M. *Chem. Mater.* **1993**, *5*, 835.
(17) Lemmon, J.; Lerner, M. *Solid State Commun.* **1995**, *94*, 533.
(18) Nazar, L. F.; Wu, H.; Power, W. P. *J. Mater. Chem.* **1995**, *5*, 1985.
(19) Lagadic, I.; Leaustic, A.; Clement, R. *J. Chem. Soc., Chem. Commun.* **1992**, 1396.

S0897-4756(96)00086-5 CCC: $12.00

Table 1. Basal Repeat Distances and Expansions for PEO-Containing Layered Nanocomposites

host	alkali metal	basal repeat (Å)	Δd^a (Å)	ref
montmorillonite	Na	**17.7**[b]	**8.1**	16
		13.7	4.1	
MoS_2	Li	14.5	8.4	1
$MoSe_2$	Li	15.2	8.7	7
TiS_2	Li, Na	14.2	8.5	17
TaS_2	Li	14.6	8.6	27
MoO_3	Li	**15**−**16**[b]	**8**−**9**	18, 7
		12.9	6.0	18
$MnPS_3$	K	**15.3**	**8.8**	
		11.3	4.8	
$CdPS_3$	K	**15.6**	**9.1**	
		11.4	4.9	

[a] Δd = difference between basal-repeat for the nanocomposites and unintercalated layered hosts. [b] Bold indicates the phase produced with excess polymer.

is certain about the conformation of PEO within these two-dimensional galleries: learning structural details of a highly disordered component in a solid is generally difficult; also, the samples must not contain any unincorporated polymer to avoid misinterpretation of results. Studies have included IR, NMR, electrical, and compositional analyses,[1,15,18] but many questions remain difficult to answer. Besides conformational analyses, fundamental polymer properties such as the average molecular weight can be difficult to assess within nanocomposites. Although the primary PEO structure, maintained by covalent linkages, should not be affected by nanocomposition with montmorillonite, this is not a safe assumption when chemically active hosts are involved. A more complete understanding of the nature of the PEO/inorganic adsorption interaction and how this affects polymer conformation and viscoelasticity would also be useful, because these molecular properties underlie macroscopic properties such as ionic conductivity and rheology.

One useful tool for analyzing polymer-containing nanocomposites would be a method for the quantitative removal and redissolution of the polymer, to allow for the subsequent application of standard spectroanalytical methods. The same kinetic limitation that prohibits topotactic incorporation of polymers, however, applies to their removal. Reports have appeared on the extraction of polymers from layered nanocomposites.[1,20,21] However, these either do not provide information as to the extent of polymer extraction or indicate that only a fraction of the polymer is removed. In either case, it is difficult to know whether the polymer subsequently analyzed represents that present in the nanocomposite.

In this study, we report for the first time a rapid, quantitative, and general method for extracting PEO from layered hosts. The polymer is displaced using aqueous tetraethylammonium salt under ambient conditions. The reaction with $K_x(C_2H_4O)_yM_{1-x/2}PS_3$ (M = Mn, Cd) is analyzed in detail, and kinetic effects are described.

Experimental Section

Materials. Polyethylene glycol standards ($M_w = 2 \times 10^3$, 5×10^3, and 1×10^4 D) were obtained from American Polymer Standards. PEO standards ($M_w = 4.6 \times 10^4$, 9.5×10^4, 1.7×10^5, 2.5×10^5, and 9.1×10^5 D) were obtained from Tosoh Corp. Commercial PEO (Aldrich, $M_w = 1 \times 10^5$, 9.8×10^5, and 5×10^6 D) was used for larger scale reactions. Lithiated MoS_2 was prepared by reaction of MoS_2 (Aldrich, 99%) with butyllithium (Aldrich, 1.6 M in hexane) following a standard procedure.[22] Li_xMoO_3 was prepared by reaction of MoO_3 (Aldrich, 99.5%) with $Na_2S_2O_4$ (Mallinckrodt, reagent) to afford Na_xMoO_3, and subsequent ion-exchange using a literature method.[23] Sodium montmorillonite clay (SWy-1, Clay Sources) was purified according to a procedure reported previously.[16]

MPS_3 (M = Mn, Cd) was prepared by heating high-purity Mn (99.9%) or Cd (>99.9%) with a stoichiometric amount of red phosphorus (Aldrich, 99.99%) and sulfur (Aldrich, 99.999%) in vacuo in a silica ampule at 650 or 680 °C for 1 week. The product identities and purities were determined by X-ray diffraction. The potassium hydrate intercalation compound, $K_xMn_{1-x/2}PS_3 \cdot H_2O$, was subsequently formed via reaction of $MnPS_3$ with 3 M KCl. The product was repeatedly centrifuged, washed with water, and then dried. For $CdPS_3$, this reaction was carried out in the presence of EDTA and a $NaHCO_3/Na_2CO_3$ buffer solution. A composition of $K_{0.3}Mn_{0.85}PS_3 \cdot 1.0H_2O$ was determined using TGA and K analysis.

All other reagents and solvents were of an analytical reagent grade and used without further purification.

Synthesis of Nanocomposites. The PEO/$K_xM_{1-x/2}PS_3$ (M = Mn, Cd) nanocomposites were prepared using the procedure described previously.[19] The potassium hydrate intercalates were dispersed in water using ultrasound (1.00 g/100 mL), added to aqueous PEO (0.50 g/100 mL), and stirred overnight at 40 °C. The nanocomposites were isolated by filtration, washed copiously with water to remove any unreacted polymer, and dried in vacuo at 80 °C for 48 h. PEO/MoS_2 and PEO/MoO_3 nanocomposites were prepared by exfoliation of the corresponding lithiated hosts (1.00 g/200 mL of H_2O) using ultrasound, followed by the slow addition of excess aqueous PEO (0.50 g/50 mL of H_2O). The mixtures were stirred for 2 h until a solid flocculated, and the products isolated as above. The PEO/montmorillonite nanocomposite was prepared by the addition of aqueous PEO (0.50 g/50 mL) to a dispersion of sodium montmorillonite in water (1.00 g/200 mL), with product isolation as above.

Displacement Reactions and Kinetic Studies. Aqueous dispersions of the nanocomposites were added to aqueous solutions containing at least 50-fold excess of $(CH_3)_4NBr$ (Aldrich, 97%), $(C_2H_5)_4NBr$ (Aldrich, 98%), $(C_3H_7)_4NBr$ (Aldrich, 98%), or $(C_4H_9)_4NBr$ (Aldrich, 99%). The reactants were stirred for a proscribed period, and a solid product was isolated by centrifugation, washing with water, and drying in vacuo at 80 °C. In kinetic studies, reaction times were counted from the initial combination of the alkylammonium salt solution (0.05−0.20 M, 10 mL) and aqueous nanocomposite dispersion (containing 0.035 g solids) until the product had been centrifuged (2−3 min) and the filtrate decanted. In this manner, the reaction begins with nanocomposite in dispersed form and thereby avoids a variable induction time associated with particle dispersion. Additionally, the protocol ensures that the entire interaction time with NR_4^+ was included for shorter reactions. All aqueous-phase reactions were conducted under ambient conditions.

Characterization. X-ray diffraction (XRD) powder patterns were obtained from sample films cast onto a Pyrex disk. Data were collected between 2 and 60° 2θ, at 0.02° 2θ s^{-1}, using a Siemans D5000 diffractometer and Cu Kα radiation (1.5418 Å). Infrared spectra were recorded on samples pressed into KBr disks containing 0.5 wt % samples, using a Nicolet 510P FTIR spectrometer (resolution = 2 cm^{-1}, 100 scans averaged). A spectrum of pure KBr was collected for background correction. Thermal analyses of powder samples (10−20 mg) were carried out at 10 °C/min in flowing air (50 mL/min), using a Shimadzu TGA-50 and DSC-50. Molecular weight profiles and polymer concentrations were obtained by elution of aqueous

(20) Liu, Y.; DeGroot, D.; Schindler, J.; Kannewurf, C.; Kanatzidis, M. *Chem. Mater.* **1991**, *3*, 992.
(21) Bissessur, R.; DeGroot, D.; Schindler, J.; Kannewurf, C.; Kanatzidis, M. *J. Chem. Soc., Chem. Commun.* **1993**, 687.
(22) Dines, M. *Mater. Res. Bull.* **1975**, *10*, 287.
(23) Thomas, D.; McCarron, E. *Mater. Res. Bull.* **1986**, *21*, 945.

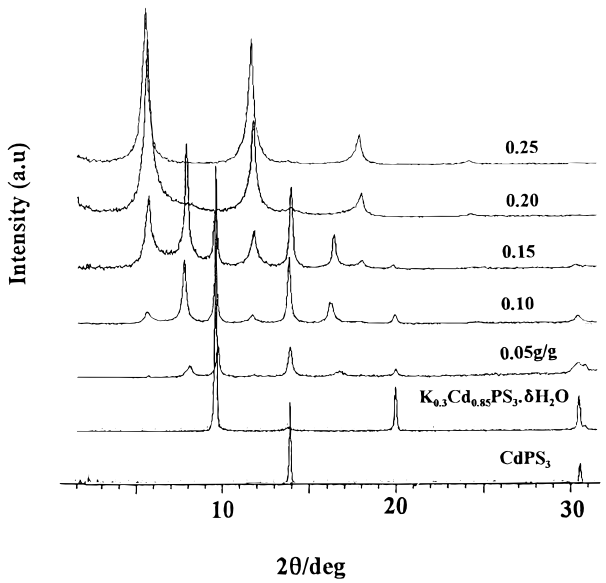

Figure 1. XRD powder patterns for products obtained by reaction aqueous PEO with $K_{0.3}Mn_{0.85}PS_3 \cdot H_2O$ in the stoichiometric range 0−0.30 g PEO/g of $K_{0.3}Mn_{0.85}PS_3 \cdot H_2O$.

polymer solution (20 μL) through a series of two ultrahydrogel linear columns (Waters) and a Waters R401 differential refractometer at 0.80 mL/min. Elution time and peak intensity calibrations were determined using PEO standards ranging from 2×10^3 to 9.1×10^5 D. A linear fit ($R^2 > 0.99$) was obtained for the relation log M_p = [−0.358 × elution time (min)] + 11.64. Elemental analyses for CHN were performed by Desert Analytics Laboratory, Tucson, AZ, potassium content was determined by flame spectrophotometry using a standard procedure.

Results and Discussion

PEO Incorporation in MPS_3. The MPS_3 structures are unique in that a wide range of intercalation chemistry exists where intercalating cations are exchanged for the host metal, rather than intragallery ion exchange or redox intercalation.[24] In this manner, a potassium intercalate is prepared simply by reaction of the MPS_3 structure with aqueous KCl. The further reaction of $K_{0.3}M_{0.85}PS_3$ (M = Mn, Cd) thus prepared with an aqueous solution of high-molecular-weight PEO results in the uptake of PEO and a further increase in the stacking dimension. With the PEO reaction stoichiometry at 0.05 g/g of $K_{0.3}Cd_{0.85}PS_3$, diffraction peaks indicate the presence of both the unreacted potassium hydrate and a phase with a stacking repeat distance of 11.4 Å (Figure 1). The latter dimension corresponds to an expansion in the stacking dimension, Δd, of 4.9 Å, compared with $CdPS_3$. When the PEO reaction stoichiometry is increased to 0.10 g/g, the content of expanded phase increases. At higher polymer stoichiometries this phase is reduced and a new expanded phase appears with stacking repeat distance of 15.6 Å (Δd = 9.1 Å). The unreacted $K_{0.3}Cd_{0.85}PS_3 \cdot \delta H_2O$ is no longer evident when the reaction stoichiometry exceeds 0.20 g/g.

These data are consistent with the accommodation of PEO as either a monolayer or bilayer between the MPS_3 sheets. Under the conditions studied, the monolayer nanocomposite is not obtained in pure form but appears in combination with either the unreacted potassium hydrate, the bilayer phase, or both. The XRD patterns do not evolve after the solid product precipitates, which suggests that the polymer cannot diffuse to provide an even distribution once the nanocomposites form. Similar results, showing expansions of 4.8 or 8.8 Å, are obtained for the interaction of PEO with $K_{0.3}Mn_{0.85}PS_3$. Observations of both monolayer and bilayer phases for PEO incorporation, with Δd of ∼4−6 and ∼9 Å, respectively, have been noted in montmorillonite and MoO_3 (Table 1).

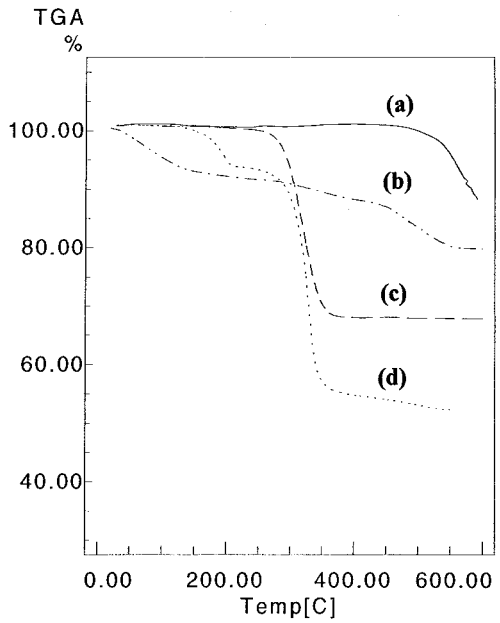

Figure 2. TGA data for (a) $MnPS_3$, (b) $K_{0.3}Mn_{0.85}PS_3 \cdot H_2O$, (c) $K_{0.3}Cd_{0.9}(C_2H_4O)_yPS_3$, and (d) $K_{0.2}(C_2H_4O)_{2.3}Mn_{0.9}PS_3$. The heating rate is 10 °C/min.

Thermogravimetry of the bilayer phase, obtained using a reaction stoichiometry of 0.30 g PEO/g of $K_xM_{1-x/2}PS_3$, shows mass losses of 7% and 1% for M = Mn and Cd, respectively, below 200 °C, which is ascribed to dehydration (Figure 2). A mass loss of 39% (M = Mn) and 32% (M = Cd) is centered at 320 °C in each sample, within the expected decomposition range for PEO. The organic content derived from the higher temperature losses are 5−10% larger than those obtained from elemental analyses, which suggests some degradation of the inorganic layered structure below 500 °C. Although the parent phases are stable to 500 °C in air, the potassium hydrate intercalate shows a mass loss of approximately 10% between 300 and 500 °C. TGA was therefore used only to set water content, and CHN and K analyses used for organic content. The nanocomposite stoichiometry was thereby determined to be $K_{0.2}(C_2H_4O)_{2.3}Mn_{0.9}PS_3 \cdot 1.2H_2O$ [calcd C = 17.9, H = 3.7, N = 0.0, K = 2.5; found C = 18.0, H = 3.1, N = 0.0, K = 2.4%]. This agrees with results communicated by Lagadic et al.,[19] who found representative stoichiometries of $K_{0.20}(C_2H_4O)_{2.14}Mn_{0.88}PS_{3.00}$ and $K_{0.27}(C_2H_4O)_{1.9}Cd_{0.84}PS_{3.0}$.

Displacement Reactions Using Aqueous $(C_2H_5)_4NBr$. The reaction of $K_{0.2}(C_2H_4O)_{2.3}Mn_{0.9}PS_3$ with an aqueous solution of tetraethylammonium bromide results in the rapid, quantitative, and irreversible displacement of both PEO and alkali-metal cations to form the alkylammonium intercalate. An XRD pattern of the product after reaction for 1−2 h shows the stacking repeat distance to decrease from 15.4 to 11.2 Å, with

(24) Clement, R. *J. Chem. Soc., Chem. Commun.* **1980**, 647.

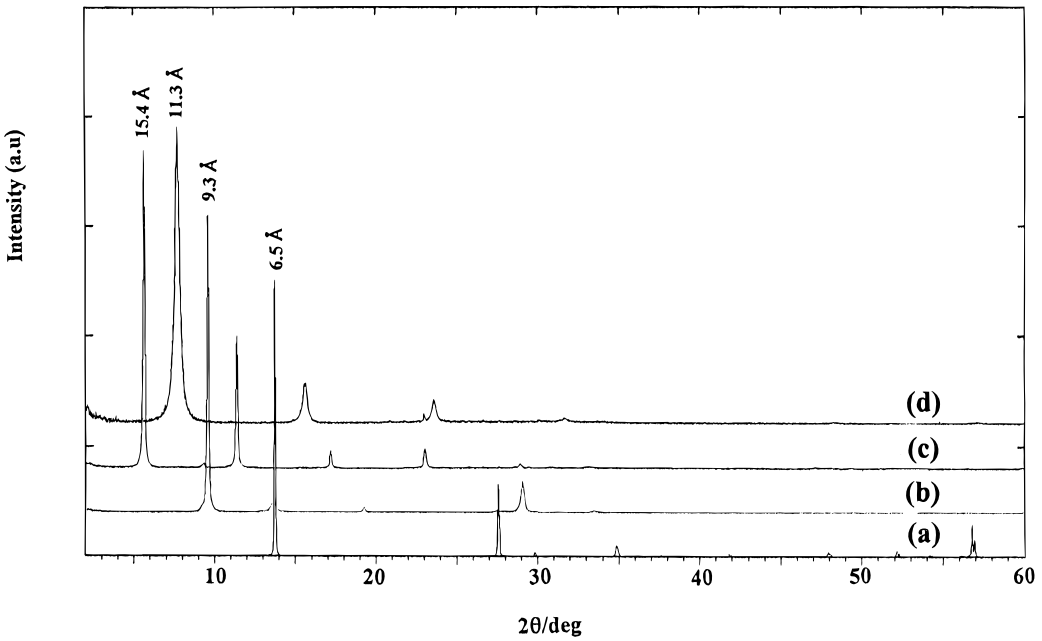

Figure 3. XRD powder patterns for (a) $MnPS_3$, (b) $K_{0.3}Mn_{0.85}PS_3 \cdot H_2O$, (c) $K_{0.2}(C_2H_4O)_{2.3}Mn_{0.9}PS_3$, and (d) $[(C_2H_5)_4N]_{0.3}Mn_{0.85}PS_3$.

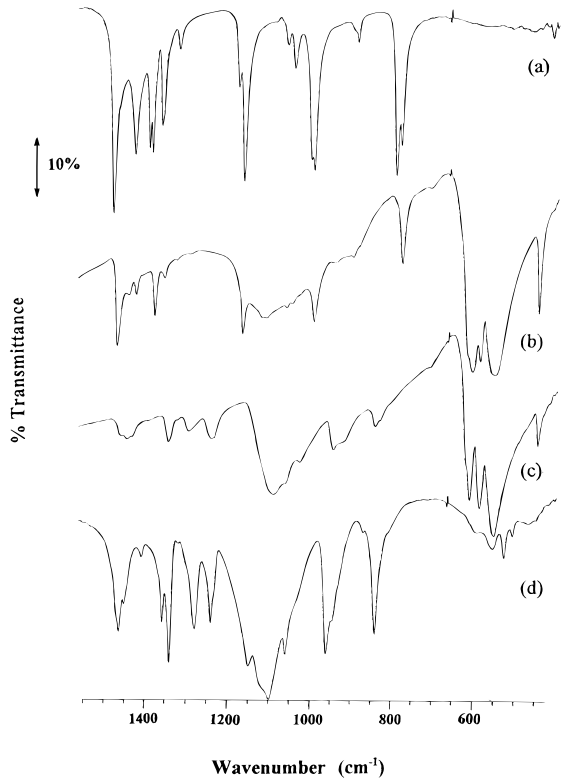

Figure 4. IR spectra (from pressed KBr disks) of (a) $(C_2H_5)_4NBr$, (b) $[(C_2H_5)_4N]_{0.3}Mn_{0.85}PS_3$, (c) $K_{0.2}(C_2H_4O)_{2.3}Mn_{0.9}PS_3$, and (d) PEO.

no other phases evident (Figure 3). This XRD pattern is indistinguishable from others obtained either by displacement of linear poly(ethylenimine) from $MnPS_3$ or by the direct reaction of aqueous $(C_2H_5)_4NBr$ with $MnPS_3$. Subsequent reactions of the alkylammonium intercalate with PEO do not alter the XRD pattern or otherwise demonstrate polymer uptake, indicating that polymer displacement is irreversible.

An IR spectrum for $K_{0.2}(C_2H_4O)_{2.3}Mn_{0.9}PS_3$ (Figure 4) shows the characteristic PEO absorption peaks at 1453, 1351, 1303, 1248, 1050−1150, 950, and 847 cm^{-1}. After the displacement reaction, an IR spectrum of the product has peaks characteristic of the alkylammonium ion. The spectrum is readily distinguished from that of the polymer-containing nanocomposite due to strong absorptions associated with the C−N stretch (1481 cm^{-1}) and terminal $-CH_3$ (1389, 1174, and 783 cm^{-1}).[25]

Thermogravimetric analyses of the tetraethylammonium intercalates obtained (a) by direct reaction of $(C_2H_5)_4NBr$ with $MnPS_3$ and (b) by displacement of PEO, provide a water content of 2 (a) and 6% (b) and losses of 35 and 41% centered at 310 °C. Although the traces are similar in form, the thermolysis of the inorganic structure overlaps with organic decomposition and the data are used for evaluation of water, but not organic, content. The product stoichiometry is $[(C_2H_5)_4N]_{0.3}Mn_{0.85}PS_3 \cdot 0.8H_2O$ [calcd C = 12.7, H = 3.3, N = 1.8, K = 0.0; found C = 13.1, H = 2.5, N = 1.8, K = 0.3%]. This composition is very similar to that reported for the compound prepared directly from reaction of $MnPS_3$ with $(CH_3)_4NCl$, $[(CH_4)_4N]_{0.32}Mn_{0.84}PS_3 \cdot 0.9H_2O$[26] and reflects some additional ion exchange of alkylammonium for Mn^{2+} during the reaction displacement reaction.

Polymer Characterization by GPC. A gel permeation chromatograph of the solution containing PEO displaced from $K_{0.2}(C_2H_4O)_{2.3}Mn_{0.9}PS_3$ shows that M_p (1.7×10^5 D) is essentially unchanged from the original polymer standard (Figure 5). The peak becomes asymmetric, however, with increased intensity on the longer-elution side, indicating some scission products in the displaced polymer. Does the polymer scission occur during nanocomposite formation, within the solid nanocomposite, or during (or after) the displacement reaction? GPC traces for the displaced polymer do not evolve with increased stirring time with alkylammonium. Similarly, the traces obtained for the displaced polymer are independent of the nanocomposite age.

(25) Theng, B. K. G. *The Chemistry of Clay-Organic Reactions*; John Wiley: New York, 1974.
(26) Evans, J.; O'Hare, D.; Clement, R. *J. Am. Chem. Soc.* **1995**, *117*, 4595.

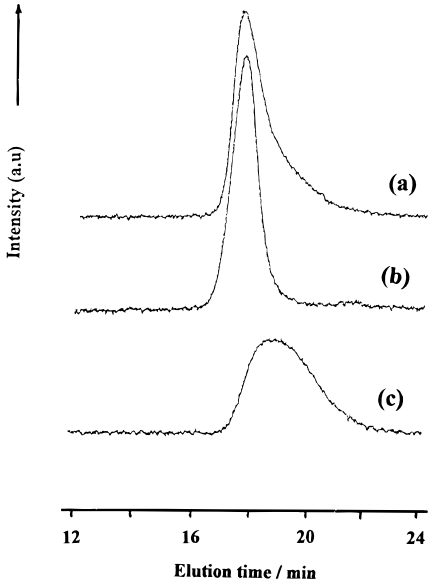

Figure 5. GPC traces for 0.2 wt % solutions (a) following reaction of aqueous $(C_2H_5)_4NBr$ with $K_{0.2}(C_2H_4O)_{2.3}Mn_{0.9}PS_3$, (b) of PEO standard ($M_w = 1.7 \times 10^5$ D), and (c) following reaction of PEO with $K_x(H_2O)_yMPS_3$. Total peak areas are similar for all traces.

These observations suggest that polymer scission occurs during the initial preparation.

Some hydrogen sulfide can be detected when $K_{0.3}Mn_{0.9}PS_3$ reacts with aqueous PEO (though not during the displacement reaction), and scission therefore may be related to nucleophilic attack of HS^- at the etheric carbon during PEO incorporation:

$$H_2S + RCH_2CH_2OCH_2CH_2R' \rightarrow RCH_2CH_2SH + HOCH_2CH_2R' \quad (1)$$

A chromatograph of the solution after the initial reaction with $K_{0.3}Mn_{0.85}PS_3$ (*5c*) provides an interesting result. The unincorporated PEO exhibits scission to a far greater extent than the displaced PEO, with M_p reduced to 1.30×10^5 in the former. The trace obtained for the excess PEO solution also resembles the difference of traces obtained for the displaced and standard PEO. These observations lead to the conclusion that polymer scission occurs in forming the nanocomposite. On the basis of the proposed mechanism, it appears this effect will be restricted to certain polymers and hosts and might even be avoided by using a scavenger for hydrogen sulfide.

A correlation of GPC peak area vs PEO concentration for standard solutions and the displaced polymer provides 0.38 ± 0.03 mmol of (C_2H_4O) displaced, as compared with 0.36 mmol in the sample of $K_{0.2}(C_2H_4O)_{2.3}Mn_{0.9}PS_3 \cdot 1.2H_2O$. On this basis, and the XRD and IR results described above, we conclude that the polymer displacement is quantitative.

Displacement Reactions with Other Layered Hosts. Rapid and quantitative displacement of PEO can also be effected with other layered hosts. Figure 6 illustrates the XRD patterns obtained following reaction between aqueous $(C_2H_5)_4NBr$ and PEO-containing nanocomposites with Li_xMoS_2, $K_{0.3}Cd_{0.85}PS_3$, Na−montmorillonite, or Li_xMoO_3. In each case, the basal repeat distance decreases by ∼3−4 Å, consistent with the

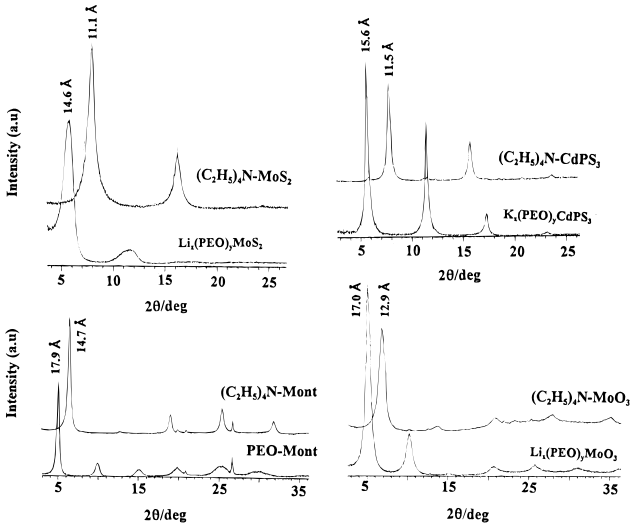

Figure 6. XRD powder patterns for PEO-containing nanocomposites and products following reaction with aqueous $(C_2H_5)_4NBr$: (a) MoS_2, (b) $CdPS_3$, (c) montmorillonite, and (d) MoO_3.

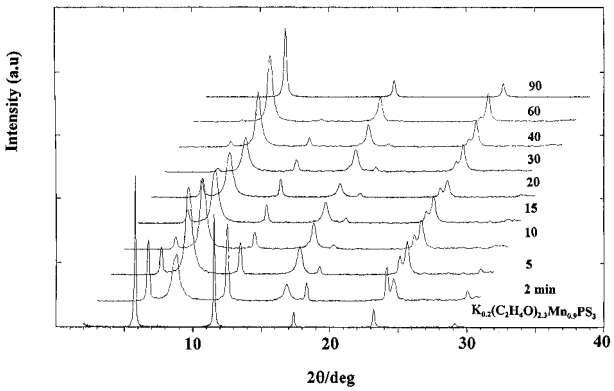

Figure 7. XRD powder patterns for products obtained from 0.15 M $(C_2H_5)_4NBr$ and $K_{0.2}(C_2H_4O)_{2.3}Mn_{0.9}PS_3$ (using M_w(PEO) $= 5 \times 10^6$ D) after reaction times indicated.

displacement of PEO bilayer and associated alkali-metal cations by tetraethylammonium.

Displacement Kinetics. A series of XRD traces corresponding to the product of 0.15 M $(C_2H_5)_4NBr$ and $K_{0.2}(C_2H_4O)_{2.3}Mn_{0.9}PS_3$ (PEO $M_w = 5 \times 10^6$ D) illustrates the rapid decrease in peak intensities for the nanocomposite ($d = 15.4$ Å) and simultaneous increases in peaks associated with the alkylammonium intercalate ($d = 11.2$ Å, Figure 7). The unconverted solid fraction is determined using

$$\chi(t) = \frac{I_{001,\text{reactant}}}{I_{001,\text{reactant}} + I_{001,\text{product}}} \quad (2)$$

where I_{001}'s correspond to (001) reflection peak intensities for the reactant, $K_{0.2}(C_2H_4O)_{2.3}Mn_{0.9}PS_3$, or product, $[(C_2H_5)_4N]_{0.3}Mn_{0.85}PS_3$, and $\chi(t)$ provides the fraction of unconverted solid in each XRD pattern. The displacement reaction involves two intercalation compounds of the same host with guests of similar densities, so differences in X-ray scattering factors should be small. The extent of reaction, $1 - \chi$, will therefore range between 0 and 1.

Since the reaction occurs in an aqueous medium, each sample pellet is prepared separately. In this analysis, an internal scaling factor is provided by the sum of

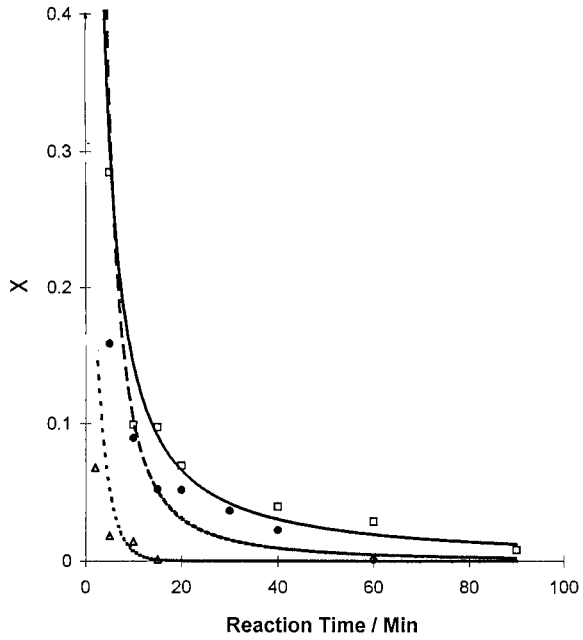

Figure 8. Residual $K_{0.2}(C_2H_4O)_{2.3}Mn_{0.9}PS_3$ content (χ) vs reaction time for products obtained from 0.15 M $(C_2H_5)_4NBr$ and $K_{0.2}(C_2H_4O)_{2.3}Mn_{0.9}PS_3$ with M_w(PEO) = (□) 5×10^6, (●) 9×10^5, and (△) 1×10^5 D. χ is determined according to eq 2.

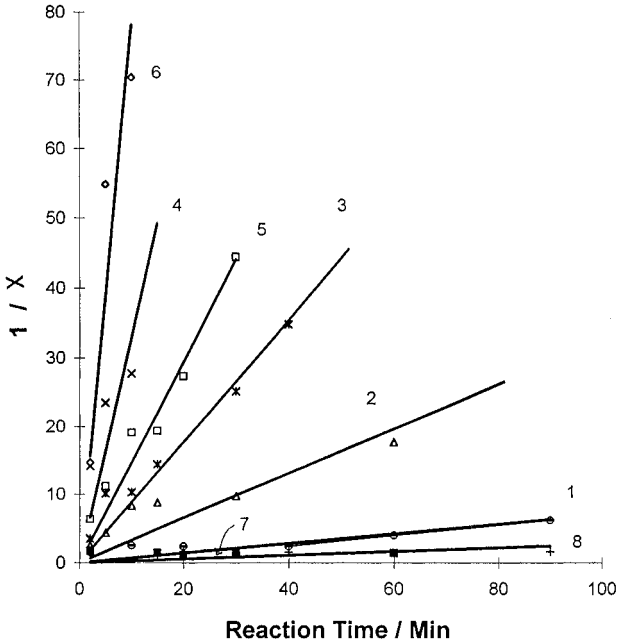

Figure 9. $1/\chi$ vs time for reactions of aqueous R_4NX with $K_{0.2}(C_2H_4O)_{2.3}Mn_{0.9}PS_3$ with various alkylammonium ions and concentrations and polymer molecular weights. Specific conditions and calculated pseudoreaction rates are in Table 2.

reactant and product peak intensities. The scaling factor assumes a constant total diffracted intensity, and is therefore approximate, but should suffice for the general comparison of reaction rates. The more usual relation employed to evaluate reaction progress, $\alpha = I_{001,obs}/I_{001,\infty}$, where $I_{001,\infty}$ reflects the peak intensity for pure product,[27] cannot be used because this diffraction intensity will vary for each sample pellet.

When the calculated values for χ are plotted against time, the displacement reactions at $[(C_2H_5)_4N^+] = 0.15$ are seen to go to completion in 15 min to 2 h (Figure 8). The plots generated under a variety of reaction conditions are linearized by taking $1/\chi$ vs time (Figure 9), and line slopes indicate pseudoreaction rates (Table 2). A strong correlation between $[(C_2H_5)_4N^+]$ and rate is evident, with a reaction order between 2 and 3, indicating a significant mechanistic role for the aqueous ion. In an insertion reaction where intercalation rate is limited principally by ion diffusion into the galleries, the rate will be independent of ion concentration in solution. This displacement reaction does not appear to proceed by such a mechanism.

The kinetic effect of the polymer molecular weight is also examined. Nanocomposites prepared from 5×10^6, 9×10^5, and 1×10^5 D PEO react at rates of 0.9, 1.5, and 7.8 min^{-1}, respectively. The increase in reaction rates by factors of 1.7 and 8.7 for the lower-molecular-weight polymers provide a rate dependence of M^{-x}, with x approximately 0.7. The expected relation between polymer molecular weight and the reaction rate for these displacement reactions is unknown. For comparative purposes, the Rouse−Bouch theory predicts $x = 1$ for polymer relaxation phenomena of unentangled chains in dilute solution.[28] The data therefore indicate that polymer dynamics play some role in the displacement mechanism, although further work will be necessary to evaluate a scaling law for any proposed mechanism.

Table 2. Effects of Alkylammonium Size and Concentration and Polymer Molecular Weight on Displacement Kinetics

no.	k (min^{-1})	R	[R_4NX] (M)	polymer M_w/D
1	0.07	C_2H_5	0.05	5×10^6
2	0.33	C_2H_5	0.10	5×10^6
3	0.89	C_2H_5	0.15	5×10^6
4	3.3	C_2H_5	0.20	5×10^6
5	1.5	C_2H_5	0.15	9×10^5
6	7.8	C_2H_5	0.15	1×10^5
7	n/a	CH_3	0.20	5×10^6
8	0.03	C_3H_7	0.20	5×10^6
9	n/a	C_4H_9	0.20	5×10^6

An unexpected result is obtained when other symmetric tetraalkylammonium cations, R_4NX (R = methyl, propyl, and butyl), are reacted with under the same conditions as $(C_2H_5)_4NBr$. The displacement reactions are slower by at least 100×, in fact, reactant and product concentrations for the $(CH_3)_4N^+$ and $(C_3H_7)_4N^+$ ions do not appear to change significantly after a small peak due to the alkylammonium intercalate appears within a few minutes. The initial product may arise from an impurity of amorphous material contained in the nanocomposite, rather than displacement of the ordered nanocomposite. No displacement reaction is observed with $(C_4H_9)_4N^+$ salt. The anomalous behavior of tetraethylammonium in these reactions contrasts with observations of direct intercalation of alkylammonium ions into MPS_3, or SnS_2, where $(CH_3)_4N^+$ is readily incorporated.[26,29] Our preliminary studies of PEO nanocomposites with montmorillonite and MoO_3 also indicate that $(CH_3)_4N^+$ and $(C_3H_7)_4N^+$ completely displace the polymer within several hours.

Why does the PEO/MPS_3 displacement reaction proceed so rapidly, and why is there such high specificity

(27) Vaia, R.; Jandt, K.; Kramer, E.; Giannelis, E. *Macromolecules* **1995**, *28*, 8080.
(28) Rouse, P. *J. Chem. Phys.* **1953**, *21*, 1272.
(29) Evans, J. S. O., private communication.

for $(C_2H_5)_4N^+$? We can provide some suggestions based on the results obtained. The PEO forms bilayers in the nanocomposite, with each PEO layer associated with one side of an MPS_3 sheet. In other systems, a consideration of the packing density of PEO layers based on the known stoichiometry indicates that they are not efficiently packed, and there is considerable unfilled volume within the polymer galleries.[1,16] The coincidence of cation and pore dimensions may lead to more favorable chemisorption of $(C_2H_5)_4N^+$ at the particle surfaces. The similarity of dimensions of $(C_2H_5)_4N^+$ and a single PEO layer is reflected in the similar basal-repeat distances of the monolayer nanocomposite and $(C_2H_5)_4N^+$ intercalate (11.4 and 11.2 Å, respectively). Ultimately, the occupancy of these sites with alkylammonium leads to coulombic repulsion and particle delamination, as illustrated in Scheme 1. Since the reaction proceeds via host delamination, the polymer layers are exposed to the solution and can be rapidly displaced. A mechanism of this type might explain both the strong rate dependence on tetraethylammonium ion concentration and also the specificity for a particular cation size. Since the MPS_3 nanocomposites possess the greatest stacking coherence with PEO (500−1000 Å, compared with 100−300 Å for PEO in other hosts), they have fewer defects and will follow this scheme more closely.

Scheme 1

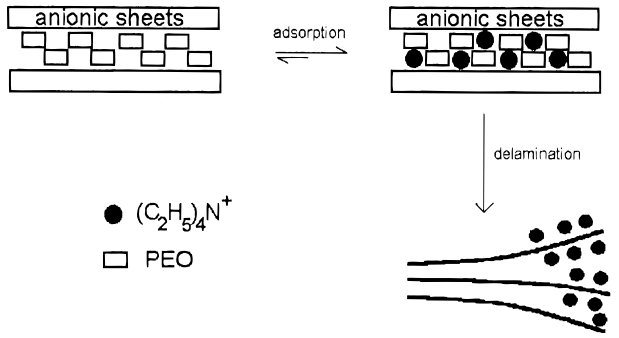

Acknowledgment. The authors gratefully acknowledge supporting Grant DMR-9322071 from the National Science Foundation. K analyses were performed by Kartik Ramachandran at O.S.U. The authors thank Dr. John Evans for helpful discussions.

CM960086O